ORIGINAL RESEARCH ARTICLE

Mild mitochondrial uncoupling induces HSL/ATGL-independent lipolysis relying on a form of autophagy in 3T3-L1 adipocytes†

Stéphane Demine,[1,†] Silvia Tejerina,[1] Benoît Bihin,[1] Thiry Marc,[2] Nagabushana Reddy,[1] Patricia Renard,[1] Martine Raes,[1] Michel Jadot,[3] and Thierry Arnould[1,*]

[1] Laboratory of Biochemistry and Cell Biology (URBC), NARILIS (Namur Research Institute for Life Sciences), University of Namur (UNamur), 61 rue de Bruxelles, 5000 Namur, Belgium

[2] Laboratory of Cell Biology, GIGA-R, University of Liège, 20 rue de Pitteurs, 4020 Liège, Belgium

[3] Laboratory of Molecular Physiology (URPhyM), NARILIS (Namur Research Institute for Life Sciences), University of Namur (UNamur), 61 rue de Bruxelles, 5000 Namur, Belgium

[†] Present address: ULB Center for Diabetes Research, Université Libre de Bruxelles, 808 route de Lennik, 1070 Brussels, Belgium

†This article has been accepted for publication and undergone full peer review but has not been through the copyediting, typesetting, pagination and proofreading process, which may lead to differences between this version and the Version of Record. Please cite this article as doi: [10.1002/jcp.25994]

Additional Supporting Information may be found in the online version of this article.

Received 8 July 2016; Revised 6 May 2017; Accepted 8 May 2017
Journal of Cellular Physiology

DOI 10.1002/jcp.25994

* **Correspondence to**: Thierry Arnould, Laboratory of Biochemistry and Cell Biology, Namur Research Institute for Life Sciences, University of Namur, 61 rue de Bruxelles, 5000 Namur, Belgium. E-Mail: thierry.arnould@unamur.be; Tel.: +32-81-724125; Fax: +32-81-724135

Running head: Autophagy regulates lipolysis induced by mitochondria uncoupling

Grant information: S. Demine was a recipient of a doctoral fellowship from the FRIA (Fonds pour la Recherche dans l'Industrie et l'Agriculture) and N. Reddy is the recipient of a doctoral fellowship from the UNamur-CERUNA (Centre d'Etudes et de Recherches Universitaires de Namur). Confocal microscopy was performed at the Technological Platform MORPH-IM platform (Morphology and Imaging) (UNamur) and equipment was bought with the financial help of FRS-FNRS (Fonds National de la Recherche Scientifique, Brussels, Belgium). The authors are also grateful to FRS-FNRS for their financial support (Crédit de Recherche: CDR 19497337)

Abbreviations

Atg (Autophagy-related), ATGL (Adipose triglyceride lipase), BCA (Bicinchoninic acid), DMEM (Dulbecco's modified Eagle's medium), DNP (2,4-dinitrophenol), E600 (p-nitrophenylphosphate), FA (Fatty acid), FCCP (Carbonyl cyanide-4-(trifluoromethoxy)phenylhydrazone), FFA (Free fatty acid), FOXO1 (Forkhead Homeobox type O1), HSL (Hormone-sensitive lipase), LC3 (Light chain 3), LD (Lipid droplet), LIPA (Lysosomal Acid Lipase A), PKA (Protein kinase A), PPARγ (Peroxisome proliferator-activated receptor γ), TAGs (Triacylglycerols), TNFα (Tumor necrosis factor α), UCP-1 (Uncoupling protein-1).

Abstract

Obesity is characterized by an excessive triacylglycerol accumulation in white adipocytes. Various mechanisms allowing the tight regulation of triacylglycerol storage and mobilization by lipid droplet-associated proteins as well as lipolytic enzymes have been identified. Increasing energy expenditure by inducing a mild uncoupling of mitochondria in adipocytes might represent a putative interesting anti-obesity strategy as it reduces the adipose tissue triacylglycerol content (limiting alterations caused by cell hypertrophy) by stimulating lipolysis through yet unknown mechanisms, limiting the adverse effects of adipocyte hypertrophy. Herein, the molecular mechanisms involved in lipolysis induced by a mild uncoupling of mitochondria in white 3T3-L1 adipocytes were characterized. Mitochondrial uncoupling-induced lipolysis was found to be independent from canonical pathways that involve lipolytic enzymes such as HSL and ATGL. Finally, enhanced lipolysis in response to mitochondrial uncoupling relies on a form of autophagy as lipid droplets are captured by endolysosomal vesicles. This new mechanism of triacylglycerol breakdown in adipocytes exposed to mild uncoupling provides new insights on the biology of adipocytes dealing with mitochondria forced to dissipate energy.

Keywords: mitochondrial uncoupling; lipolysis; autophagy; HSL; ATGL; adipocytes; lipid metabolism; glycerol

Introduction

Obesity can be defined as an excessive storage of lipids (as triacylglycerols, TAGs) in white adipose tissue leading to a body mass index higher than 30 (Guh *et al.*, 2009). It is also often associated with other features such as dyslipidemia, hypertension, hyperinsulinemia, insulin resistance, and type 2 diabetes mellitus as well as some forms of cancer (Guh *et al.*, 2009). Obesity is mainly due to an imbalance between energy intake and energy consumption that could be caused, at least partly, by an unhealthy diet or insufficient physical exercise. However, it is also importantly influenced by an individual's multigenic background, affecting genes encoding thyroid peroxidase, peroxidasin and myelin transcription factor 1-like (deletions) (Doco-Fenzy *et al.*, 2014), leptin and leptin receptor (mutations) (Clement *et al.*, 1998; Wabitsch *et al.*, 2015), or Forkhead box A3 (single nucleotide polymorphism) (Adler-Wailes *et al.*, 2015). Microbial factors, such as the composition of the gut microbiota, are also known to influence obesity onset (Kong *et al.*, 2014).

It has been clearly demonstrated that a loss of 5–10 % in lipid content can alleviate obesity-linked complications in humans (Jones *et al.*, 2007). An attractive strategy to limit fat accumulation and stimulate energy expenditure in adipose tissues (Harper *et al.*, 2001) involves triggering a low-grade/controlled/targeted and chronic (mild) mitochondrial uncoupling in these tissues, as long as it is accompanied by the stimulation of free fatty acid (FFA) β-oxidation in other tissues such as heart, muscles, liver kidney, and brown adipose tissue (Harper *et al.*, 2001). In 3T3-L1 adipocytes, it has been shown that a mild uncoupling of mitochondria limits fat accumulation by reducing the expression of pyruvate carboxylase, limiting TAG and fatty acid (FA) synthesis (De Pauw *et al.*, 2012) and increasing lipolysis (Si *et al.*, 2007; Tejerina *et al.*, 2009). However, the molecular mechanisms triggered by mitochondrial uncoupling leading to the activation of lipolysis remain poorly understood.

Lipid droplet (LDs) are composed of a core of neutral lipids surrounded by a lipid monolayer containing several "coat proteins" such as perilipin 1 (perilipin A), perilipin 2 (adipophilin), perilipin 3 (Tail-Interacting Protein of 47 kDa), perilipin 4 (S3-12), and perilipin 5 (Lipid Storage Droplet Protein 5). The biology of LDs has been extensively reviewed (Thiam *et al.*, 2013; Walther and Farese, 2012). Lipolysis allows the mobilization of FFAs from TAGs stored in LDs (Sun *et al.*, 2011). Activation of this metabolic pathway can be observed in adipocytes in different conditions, including following exposure to tumor necrosis factor-α (TNFα) (Yang *et al.*, 2011) or in response to the stimulation of β3-adrenergic receptors (Schimmel, 1976). Interestingly, rats exposed to acute hypoxia exhibit increased FFA blood levels, suggesting the activation of lipolysis when a deprivation of oxygen is observed (Yin *et al.*, 2009), a condition also found during the expansion of adipose tissues in obese individuals (Hosogai *et al.*, 2007).

Three major forms of lipolysis have been identified to date. The first form is the "classical lipolysis", mainly fulfilled by specific neutral lipases, namely hormone-sensitive lipase (HSL) and adipose triglyceride lipase (ATGL) (Lafontan *et al.*, 2009), which are mainly cytosolic at the basal state. However, in response to the activation of β3-adrenergic receptors, protein kinase A (PKA) phosphorylates both perilipin 1 and HSL (Anthonsen *et al.*, 1998; Souza *et al.*, 2002; Tansey *et al.*, 2003), leading to the recruitment and activation of HSL at the surface of the LDs. In addition, phosphorylation of perilipin 1 leads to the release of Comparative Gene Identification-58, an ATGL co-activator (Lass *et al.*, 2006; Sahu-Osen *et al.*, 2015), from perilipin 1. Together, HSL, ATGL, and monoacyl glycerol lipase mobilize FFAs from TAGs (Lass *et al.*, 2011).

A second mechanism allowing mobilization of FFAs is the macroautophagy of LDs (lipophagy), a process identified both *in vitro* and *in vivo* in rat RALA255-10G hepatocytes exposed to oil-rich medium and in liver-specific conditional autophagy-related 7 (*Atg7*)

knock-out mice, respectively (Demine *et al.*, 2012; Singh *et al.*, 2009a). In these conditions, the recruitment of light chain 3 (LC3), an autophagosomal marker, to the LD is observed, initiating the formation of autophagosomal engulfment of the LD in an Atg7-dependent manner and allowing the fusion with lysosomes in which lipolytic enzymes digest the TAG contained in LDs (Demine *et al.*, 2012; Singh *et al.*, 2009a). So far, the existence of lipophagy has been confirmed in hepatocytes (Singh *et al.*, 2009a) (Martinez-Lopez *et al.*, 2016), white (Lettieri Barbato *et al.*, 2013) and brown (Martinez-Lopez *et al.*, 2016) adipocytes, pancreatic β cells (Pearson *et al.*, 2014), T cells (Hubbard *et al.*, 2010), or neurons (Kaushik *et al.*, 2011). Moreover, autophagy is not only involved in lipid droplet disposal in adipocytes but also plays a key role during adipogenesis. Indeed, silencing of *Atg5* or *Atg7* expression in 3T3-L1 adipocytes leads to the limitation of fat accumulation and increases the expression of brown adipocyte molecular markers such as uncoupling protein-1 (UCP-1) (Singh *et al.*, 2009b). These effects have also been observed in *Atg7* knock-out mice (Zhang *et al.*, 2009). Chaperone-mediated autophagy (CMA) could also play a role in the regulation of autophagy. Indeed, perilipins 2 and 3 are substrates of CMA (Kaushik *et al.*, 2015). During starvation, an increase in CMA rate leads to a progressive degradation of both proteins in mouse fibroblasts, which allows a facilitated recruitment of ATGL and macroautophagy machinery to the surface of the lipid droplets and thus, increase lipolysis rate (Kaushik and Cuervo, 2015; Kaushik *et al.*, 2016). At the opposite, the inhibition of CMA limits the lipid droplet degradation and lipolysis activation (Kaushik and Cuervo, 2015). This process seems to be dependent on the phosphorylation of perilipin 2 by AMPK (Kaushik and Cuervo, 2016).

Finally, a third mechanism relies on a form of microautophagy. This form of autophagy involves the direct capture of small cytosolic portions by the lysosomes and can either be non-selective or selective for some organelles, as demonstrated for mitochondria (Lemasters, 2014), peroxisomes (Sakai *et al.*, 1998), nuclei (Dawaliby *et al.*, 2010), and ribosomes (Kraft

et al., 2008). Unfortunately, the machinery regulating this autophagy pathway remains poorly documented in mammals. Very recently, LD degradation by microautophagy was also reported in yeast incubated in oil-rich medium (van Zutphen *et al.*, 2014).

Herein, the molecular mechanisms involved in lipolysis induced by a mild uncoupling of mitochondria triggered by carbonyl cyanide-4-(trifluoromethoxy)phenylhydrazone (FCCP) were analyzed in 3T3-L1 adipocytes. The role of HSL and ATGL in FCCP-induced glycerol release was first excluded, followed by an assessment of the putative participation of macroautophagy in glycerol release from adipocytes exposed to FCCP. Despite an apparent increase in macroautophagy flow in adipocytes exposed to mitochondrial uncoupling, it was found that inhibition of macroautophagy by bafilomycin A1 (Baf A1) or by the silencing of expression *Atg5* or *Atg7*, key molecular actors of autophagy, did not prevent the lipolysis induced by FCCP. Finally, a direct capture of LDs by lysosomes was observed. The role of autophagy in this process was confirmed by the fact that both valinomycin, an inhibitor of microautophagy (Kunz *et al.*, 2004), and lysosome poisoning induced by several inhibitors, totally inhibit FCCP-induced glycerol release.

Materials and methods

Chemicals

Bafilomycin A1, chloroquine, dodecyltriphenylphosphonium (C12TPP), dexamethasone, db-cAMP (dibutyryl-cyclic AMP), E64d, FCCP, free glycerol and TAG determination kit, insulin, ionomycin, isoproterenol, NH_4Cl, p-nitrophenylphosphate (E600), sucrose were purchased from Sigma. The bicinchoninic acid (BCA) Pierce protein determination kit and siRNAs targeting *Atg5*, *Atg7* or non-targeting (non-targeting pool, NTP) were obtained from Thermo Scientific. Dulbecco's Modified Eagle's Medium (DMEM) and fetal bovine serum

(FBS) were purchased from Gibco. Valinomycin was obtained from Santa Cruz Biotechnology.

Cell culture and differentiation

Murine 3T3-L1 preadipocytes purchased from the American Type Culture Collection were differentiated using a pro-adipogenic cocktail containing insulin, dexamethasone, and db-cAMP (all from Sigma) as previously described (Vankoningsloo *et al.*, 2006). Briefly, after 12 days of differentiation (>90 % of differentiated cells), adipocytes were incubated for an extra 3 days in the presence of 0.5 µM FCCP (Sigma) diluted in DMEM containing 10 % FBS (defined as the culture medium herein). Media were renewed every 2 days during the differentiation program and every day when molecules were added. Further treatments are indicated in the legends of respective figures.

Cleared cell lysate preparation and protein content determination

Following the different incubations, cells were rinsed twice with ice-cold phosphate buffer saline (PBS) and lysed for 30 min in 150 µL of ice-cold lysis buffer (20 mM Tris (Merck); pH 7.4, 150 mM NaCl (Merck), 1 mM EDTA (Merck), 1 % Triton X-100 (Sigma)) as previously described (Vankoningsloo *et al.*, 2005). Cleared cell lysates were prepared by centrifugation (13,000 rpm, 15 min, 4 °C; Eppendorf 5415R centrifuge). Sample protein concentration was determined through the BCA Pierce method.

Total lipid extraction, triacylglycerol content, glycerol and FFA release assays

Cells were rinsed once with 5 mL of PBS, scraped into 1 mL of PBS, and total lipids were extracted by the addition of 7.4 mL of chloroform/methanol (Sigma/Acros, respectively) (v/v 1:2). Samples were shaken for 15 min at room temperature (RT) and the extraction was continued by the addition of 2.5 mL of chloroform (Merck) and 2.5 mL of 1 M NaCl (Merck).

The different phases were separated by centrifugation (1125 *g*, 11 min, RT, Eppendorf 5810R centrifuge). The polar phase was collected and the solvent was evaporated to dryness under nitrogen flow. Lipids were finally solubilized in 50 µL of ethanol (Merck) and stored at –20 °C before use. Glycerol or TAG concentrations were assessed either in the 24-hour-old conditioned culture media of differentiated cells incubated for a total of 3 days in the presence or absence of 0.5 µM FCCP (Sigma) or in lipid extracts by using the free glycerol and TAG determination kit (Sigma) according to the manufacturer's instructions. In the same conditioned culture media, the release of FFAs was quantified using FFA assay kit (Sigma) according to the manufacturer's instructions. Results were expressed in µg of glycerol, µg of TAG or µmole of FFAs and were then normalized for protein content, as determined by the BCA method.

Triglyceride lipase assay

The protocol used for triglyceride lipase activity determination was adapted from a previously published protocol (Rider *et al.*, 2011). Briefly, cells were first rinsed with 5 mL of PBS. Cell homogenates were prepared in 200 µL of buffer (25 mM HEPES (Sigma), pH: 7.4; 255 mM sucrose (Sigma), 1 mM EDTA (Merck), 1 mM DTT (Merck)) using a Dounce homogenizer (40 strokes). For each experimental condition, the protein concentration was determined through the BCA method. A volume of 100 µL containing 200 µg of proteins was prepared and incubated for 3 h at 37 °C in the presence of 100 µL of enzymatic reaction buffer (2 µCi [9-10-^{3}H(N)]-triolein (20 nM/mL; Perkin Elmer), 100 mM KH_2PO_4 (Merck), 5 % (w/v) bovine serum albumin (Sigma), phosphatidylcholine-phosphatidylethanolamine (w/w: 3/1; Sigma)). The enzymatic reaction was then stopped by the addition of H_3BO_4 (1.05 mL; pH 10.5; Merck) and FFAs were extracted by the addition of methanol/chloroform/heptane (3.25 mL; v/v/v: 10/9/7). Samples were then centrifuged (20 min, 2,000 rpm, Jouan B3.11

centrifuge), the supernatant containing FFAs was removed, and the radioactivity was counted on 1 mL sample aliquots in a scintillation counter (Beckman Coulter).

Western blot analyses

Fluorescence-based western blot analyses (Delaive *et al.*, 2008) were performed on 25 µg of proteins from cleared cell lysates that were previously resolved by SDS-PAGE (Bio Rad) and transferred on PVDF membranes (Millipore). The acrylamide percentages, antibodies, manufacturers, and concentrations used are summarized in **Supp. Table 1**. The fluorescence emitted by the antibodies was detected using a Li-Cor scanner (Odyssey) and quantified with the Odyssey software. The data normalization method is detailed in the legends of corresponding figures.

Electroporation

At the end of the incubations, cells were rinsed twice with 15 ml of PBS (Lonza), harvested by 5 ml of trypsin/EDTA (Gibco) for 10 min at 37 °C and diluted into a final volume of 10 ml of culture medium. Cell density was evaluated using a Neubauer chamber (Marienfield). Volumes containing 2.10^6 adipocytes were prepared and centrifuged for 5 min at 1,000 rpm (Eppendorf 5702). Media were removed and cell pellets were collected into 100 µl of Nucleofector solution Kit L (Lonza). A solution containing siRNAs directed against 20 nM Atg5, 100 nM Atg7, or control "non-targeting" siRNAs (120 nM) (OnTarget Plus SmartPool, Thermo) was added. Cells were then electroporated (Nucleofector equipment; Lonza) according to the manufacturer's instructions. Immediately after the electroporation, a volume of 1 ml of culture medium containing 5 µg/ml insulin (Sigma) was added to the cells that were seeded in 6-well plates (Corning). After 24 h of recovery, media were renewed and the cells were treated according the conditions described in the legend of the corresponding figure.

Analysis of the co-localization of lysosomes and LDs by confocal microscopy

Cells were differentiated and incubated with or without FCCP in the presence or in the absence of Baf A1. Cells were next incubated for 1 h with 50 nM of LysoTracker Red DND-99 (Life Technologies) diluted into regular culture medium with or without 0.5 µM of FCCP. Cells were then fixed with 4 % paraformaldehyde diluted in PBS (Sigma) for 10 min at room temperature and incubated for 30 min with PBS containing 20 µg/mL of BODIPY 493/503 (Life Technologies). Immunofluorescence was also used in order to analyze the co-localization of these organelles. First, cells were fixed with methanol/acetone for 15 min at RT, incubated for 2 h at RT into PBS containing 1% BSA and the antibodies targeting LAMP-1 (lysosomal marker), perilipin 1 (lipid droplet marker) or LC3 (autophagosomal marker) and 1 h at RT with corresponding secondary antibodies (**Supp. Table 1**). The staining of nuclei was performed by incubating the cells with 12.5 µM TO-PRO 3 iodide (Life Technologies) for 30 min. Cells were finally observed using a confocal microscope (Leica TCS SP5) (LysoTracker Red λ excitation: 577 nm, λ emission: 590 nm; BODIPY λ excitation: 480 nm, λ emission: 515 nm; TO-PRO 3 λ excitation: 642 nm, λ emission: 661 nm; Alexa Fluor 488: λ excitation: 495 nm, λ emission: 519 nm; Alexa Fluor 568 λ excitation: 578 nm, λ emission: 603 nm). Co-localization between organelles was assessed in cells randomly chosen by measuring the Pearson correlation coefficient using the ImageJ plugin Coloc2 as previously described (Adler *et al.*, 2010; Dunn *et al.*, 2011).

Transmission electron microscopy (TEM) analysis

At the end of the different incubations, cells were then fixed for 1 h in a 0.1 M sodium cacodylate buffer (pH 7.4; Sigma) containing 2.5 % glutaraldehyde (v/v; Santa Cruz Biotechnology) and post-fixed for 30 min with 2 % (w/v) osmium tetroxide in the same buffer. Samples were then dehydrated at room temperature through a graded ethanol series (70 %, 96 %, and 100 %) and embedded in Epon for 48 h at 60 °C. Ultrathin sections (70 nm

thick) were obtained by using an ultramicrotome (Reichert Ultracut E) equipped with a diamond knife (Diatome). The sections were mounted on copper grids coated with collodion and contrasted with uranyl acetate and lead citrate for 15 min each. The ultrathin sections were observed under a JEM-1400 transmission electron microscope (Jeol) at 80 kV and micrographies were taken with an 11 MegaPixel bottom-mounted TEM camera system (Quemesa, Olympus). At least 20 adipocytes for each condition (control adipocytes and FCCP-treated cells) were observed in order to allow quantification. The number of endolysosomal vesicles and the number of interactions between these vesicles and LDs were manually determined in each cell.

Cell fractionation, lysosomal TAG content, and glycerol release assay

Lysosomal enriched fractions were prepared as previously described (Graham, 2002; Wattiaux *et al.*, 1978). Briefly, at the end of the incubations, cells (corresponding to 150 cm^2 per experimental condition) were rinsed twice with 15 mL of ice-cold PBS and homogenized into 2 mL of homogenization buffer (255 mM sucrose (Sigma), 20 mM HEPES (Sigma), 1 mM EDTA (Merck); pH 7.4) with a Dounce homogenizer (40 strokes). Nuclei were first pelleted by centrifugation (1,000 *g*, 10 min, 4 °C; Eppendorf 5810R centrifuge). A mitochondria-enriched fraction was prepared by ultracentrifugation (7,000 rpm, 10 min, 4 °C; Beckman Coulter L7 centrifuge), followed by a lysosome-enriched fraction by ultracentrifugation of the supernatant (25,000 rpm, 10 min, 4 °C; Beckman Coulter L7 centrifuge), and diluted into 1 mL of a buffer optimized for lysosomal preservation (0.3 M sucrose (Sigma), 10 mM MOPS (Merck); pH 7.3) (Bandyopadhyay *et al.*, 2008; Cuervo *et al.*, 1997). Samples were incubated in a water bath for 1 h at 37 °C in order to allow the degradation of intralysosomal TAG. Lysosomes were finally pelleted by ultracentrifugation (25,000 rpm, 10 min, 4 °C, Beckman Coulter L7 centrifuge). Supernatants were collected and lysosomal pellets were recovered in 200 µL of lysosomal buffer. Glycerol and TAG

concentrations were determined using the free glycerol and TAG determination kit. The results were expressed in µg of glycerol or TAGs per µL of sample and were then normalized for lysosomal protein content, as determined by the BCA Pierce method.

Statistical analyses

Data from at least three independent experiments were analyzed by either a Student *t*-test, a z-test (Sprinthall, 2012) or one-way ANOVA, as mentioned in the figure legends or in the text. Tests were performed with GraphPad Prism 6 software. Means were considered statistically significant with $p<0.05$ or less.

Results

Mild uncoupling of mitochondria triggers lipolysis and decreases adipocyte TAG content

As expected, at the basal state, a low glycerol efflux from differentiated adipocytes was observed (**Fig. 1A**). Indeed, a basal lipolytic activity and constant lipid remodeling occurs in adipocytes both *in vitro* and *in vivo* (Arner *et al.*, 2011; Edens *et al.*, 1990; Jensen *et al.*, 2001). However, when 3T3-L1 murine adipocytes were incubated for 3 days with a low FCCP concentration (0.5 µM), a condition sufficient to induce a slight but significant decrease in mitochondrial membrane potential while largely preserving cell viability (**Sup. Fig. 1A, 1B**) as previously described (Tejerina *et al.*, 2009), the release of glycerol is significantly increased (**Fig. 1A**). It must be noted that the magnitude of the FCCP effect was variable (from 150 % to 300 % when compared with untreated cells). Nevertheless, in accordance with the increased glycerol release, lipid content was also significantly decreased in FCCP-treated adipocytes (**Fig. 1B and Fig. 1C**) (Tejerina *et al.*, 2009). In addition, some

FFAs generated from the TAGs breakdown during FCCP-induced lipolysis seem to be released in the extracellular conditioned culture medium (**Fig. 1D**). Mild uncoupling of mitochondrial oxidative phosphorylation is thus able to stimulate lipolysis and is associated with a decrease in adipocyte lipid content. These effects were comparable, in intensity, to the activation of lipolysis triggered by isoproterenol, a β-adrenergic agonist, or by TNFα, a pro-inflammatory cytokine (**Fig. 2A**).

Classical lipolysis, induced by either TNFα or isoproterenol, essentially depends on the activation of HSL and ATGL (Kim *et al.*, 2006; Yang *et al.*, 2011). Therefore, the abundance of these enzymes was first evaluated through fluorescence-based western blotting. Quantification of several blots revealed that the abundance of HSL was significantly decreased in FCCP-treated adipocytes (**Fig. 2B**). In addition, the enzyme did not seem to be activated by the treatment, as no increase in the phosphorylation of HSL on the serine 660, a marker of the activation and recruitment of this enzyme (Watt *et al.*, 2006), could be observed in these conditions (**Fig. 2B**). The abundance of ATGL was also decreased in these experimental conditions (**Fig. 2B**). While slightly reduced, the abundance of perlipin 1 is not statistically different in FCCP-treated cells when compared with abundance in control adipocytes (**Fig. 2B**).

Since the total protein abundance of HSL and ATGL was decreased in FCCP-treated adipocytes, the total TAG lipase activity was also assessed in these conditions. Total TAG lipase activity was significantly decreased in FCCP-treated adipocytes when compared with the activity in control adipocytes (**Fig. 2C**). In addition, the presence of E600, an inhibitor of neutral lipases such as pancreatic lipase in pigs (Maylie *et al.*, 1972), microsomal triglyceride lipase, and HSL in 3T3-L1 adipocytes (Gilham *et al.*, 2003; Wei *et al.*, 2007), inhibited the global triglyceride lipase activity in both untreated and FCCP-treated adipocytes (**Fig. 2C)**.

However, in order to determine whether cytosolic neutral TAG lipases contribute to the glycerol release by adipocytes facing a mitochondrial uncoupling, lipolysis was assessed in adipocytes exposed to FCCP in the presence or in the absence of E600. No inhibitory effect of the molecule on FCCP-induced glycerol release by adipocytes was observed (**Fig. 2A**). Furthermore, a consistent and reproducible (but unexplained) increase in glycerol release was observed in FCCP-treated cells. However, the efficiency of E600 in adipocytes was demonstrated in these cells as E600 completely inhibits glycerol release in 3T3-L1 stimulated with either isoproterenol or TNFα (**Fig. 2A**), two molecules known to trigger lipolysis by both ATGL- and HSL-dependent mechanisms (Kim *et al.*, 2006; Yang *et al.*, 2011). In summary, these experiments support the hypothesis that lipolysis in 3T3-L1 adipocytes exposed to a mitochondrial uncoupling does not rely on the activation of HSL or ATGL.

Macroautophagy is stimulated in adipocytes exposed to mitochondrial uncoupling

The putative contribution of lipophagy, an alternative form of lipid degradation (Singh *et al.*, 2009a), to the degradation of TAGs in cells facing mitochondrial uncoupling was analyzed. First, macroautophagy was evaluated by analyzing the abundance of LC3-II, an autophagosomal marker (Kabeya *et al.*, 2000), and polyubiquitin-binding protein p62/SQSTM1, a protein selectively degraded by macroautophagy (Bjorkoy *et al.*, 2005). When analyzed simultaneously, these markers allow the evaluation of autophagic flow (Klionsky *et al.*, 2016). A significant decrease in the abundance of both markers was observed in adipocytes exposed to mitochondrial uncoupling, suggesting that the rate of macroautophagy is increased in these conditions (**Fig. 3A**).

As canonical macroautophagy is dependent on both Atg5 and Atg7, two proteins traditionally considered as required for the autophagosome formation (Hanada *et al.*, 2007; Komatsu *et al.*, 2005; Tanida *et al.*, 2001), we next studied the effect of Atg5 and/or Atg7 silencing on the

glycerol released by FCCP-treated adipocytes. As expected, both siRNAs considerably reduced the protein abundance of their respective target (**Supp. Fig. 2**). However, neither the silencing of Atg5, Atg7, or both, was able to significantly decrease the glycerol release by cells incubated with FCCP when compared with adipocytes transfected with control siRNA (siNTP) (**Fig. 3B**). While a strong decrease in the abundance of these proteins is observed in siRNA-transfected cells, we cannot completely rule out the possibility that the silencing of *Atg5/Atg7* was not efficient enough to modify the macroautophagy rate as in 3T3-L1 adipocytes. Indeed, the abundance of LC3-II and p62 was unchanged in response to *Atg5* and/or *Atg7* silencing (**Fig. 3C**). However, it seems unlikely as a comparable silencing efficiency induces LC3-II accumulation in 3T3-L1 preadipocytes (**Fig. 3D)**.

Nevertheless, in order to circumvent this problem, we next tested the effects of Baf A1, a lysosomal V_0/V_1 H^+-ATPase inhibitor (Yamamoto *et al.*, 1998) reported to inhibit macroautophagy in several models (Furuchi *et al.*, 1993; Klionsky *et al.*, 2008; Yamamoto *et al.*, 1998; Yoshimori *et al.*, 1991) on lipolysis of adipocytes incubated with FCCP. While this molecule stimulates the basal glycerol release by adipocytes, it does not have any effect on FCCP-induced glycerol release in adipocytes (**Fig. 3E**), despite an apparent blockage of autophagy as suggested by the accumulation of LC3-II in this condition (**Fig. 3A**). Altogether, these results suggest that the lipolysis observed in adipocytes exposed to a mitochondrial uncoupling is independent on macroautophagy.

Lysosomes can directly degrade LDs in FCCP-treated adipocytes

As previous experiments did not allow us to draw definitive conclusions regarding the possible role of macroautophagy in the FCCP-induced glycerol release, we decided to more precisely assess the role of lysosomes in TAG breakdown occurring in adipocytes exposed to mitochondrial uncoupling by other approaches. Lysosomes and LDs were stained with

LysoTracker Red and BODIPY, specific fluorescent probes for lysosomes/acidic compartments (Fuller *et al.*, 2003) and neutral lipids (Spangenburg *et al.*, 2011), respectively. Interestingly, while co-localization events between lysosomes and LDs could be observed in both adipocytes and FCCP-treated cells (**Fig. 4A**), the occurrence of such co-localization events was significantly higher in adipocytes treated with FCCP (**Fig. 4C**). Alternatively, we used immunofluorescence and other markers in order to confirm these results. Lysosomes and lipid droplet membranes were detected using antibodies targeting LAMP-1 or perilipin 1, respectively. An increase in the number of the occurrence of co-localization events in FCCP-treated cells was also observed by using this approach (**Fig. 4B-D**). These results confirm data obtained by using LysoTracker Red and BODIPY and suggest a role for lysosomes in the breakdown of TAGs in adipocytes undergoing mitochondrial uncoupling. Interestingly, incubation in presence of Baf A1 increased the number of autophagosomes and lysosomes in both control and FCCP-treated cells, but does not significantly increase the co-localization between the organelles and the lipid droplets (**Fig. 4B-D, Supp. Fig. 4A-B**).

The co-localization between lysosomes and LDs was then assessed by TEM in FCCP-treated and untreated adipocytes. Interestingly, FCCP-treated adipocytes exhibited more endolysosomal vesicles (identified as round-shaped vesicles with numerous intraluminal vesicles). Indeed, such vesicles were found in nine out of 20 FCCP-treated cells observed (3.2 vesicles/cell) compared to five out of 20 untreated cells (($p<0.027$, binomial distribution), 2.2 vesicles per cell (NS, $p>0.05$, z-test (Sprinthall, 2012))). Moreover, a close proximity between endolysosomal vesicles and LDs was also observed in FCCP-treated adipocytes (**Fig. 5**). Some endolysosomal vesicles also contain LDs. Moreover, these vesicles had a 1–2 µm wider diameter in FCCP-treated cells when compared with untreated adipocytes, suggesting a very active process of lipid engulfment (**Fig. 5**).

In order to further delineate the putative role of lysosomes in TAG breakdown and its enhanced contribution to LD remodeling in adipocytes exposed to the mitochondrial uncoupler, the TAG content in lysosomal-enriched fractions prepared by cell fractionation from control adipocytes or FCCP-treated cells was determined (**Fig. 6A**). Indeed, mitochondrial uncoupling seemed to induce lipid accumulation in the lysosomes of FCCP-treated cells. In addition, when the lysosomes were poisoned by incubation in the presence of sucrose, Baf A1, E64d, NH_4Cl, or chloroquine, molecules known to reduce the activity of some lysosomal hydrolases, no real effect can be observed on FCCP-induced glycerol release. However, this process is almost totally abolished when these compounds are used in combination in a cocktail (**Fig. 6B**). As already observed before, some of these compounds (Baf A1 and choloroquine) significantly increase the basal glycerol release level (**Fig. 6B**).

Interestingly, as macroautophagy might not be involved in FCCP-induced lipolysis, the close proximity (and possibly fusion events) between endolysosomal vesicles and LDs suggest a possible participation of another lysosomal-dependent pathway: microautophagy. In accordance with this hypothesis, the existence of a form of microautophagy that is specific to LDs has recently been identified in yeast (van Zutphen *et al.*, 2014). Adipocytes or FCCP-treated cells were thus incubated in the presence or in the absence of valinomycin, a potassium ionophore reported to inhibit microautophagy (Kunz *et al.*, 2004). Treatment with valinomycin significantly inhibited glycerol release by adipocytes exposed to a mild uncoupling of mitochondria (**Fig. 6C**). However, valinomycin did not significantly affect glycerol release in control adipocytes (**Fig. 6C**). Interestingly, valinomycin also significantly decreases the level of colocalization between lysosomes and lipid droplets in FCCP-treated cells (**Fig. 4B-D**). These data suggest the possibility that microautophagy could be responsible, at least partially, for the rise in glycerol efflux from adipocytes incubated with FCCP.

Finally, in order to support our data, we checked that, in FCCP-treated cells, glycerol is released from a lysosomal source. Therefore, lysosomes were isolated from homogenates of adipocytes and FCCP-treated cells (incubated with or without valinomycin) by centrifugal fractionation and the organelle-enriched fractions were incubated with a buffer designed to maintain lysosomal integrity (Bandyopadhyay *et al.*, 2008). After 1 h, lysosomes were pelleted by centrifugation and the glycerol concentration was measured in the supernatants (**Fig. 6D**). The fact that more glycerol could be measured in the supernatants of lysosomal-enriched fractions prepared from FCCP-treated cells (an effect reduced when cells were incubated with FCCP in the presence of valinomycin) suggests that TAGs are broken down (releasing glycerol) by lysosomes in cells exposed to a mild uncoupling of mitochondria.

In conclusion, these results support the possibility that a form of autophagy is directly involved in the activation of lipolysis in 3T3-L1 adipocytes exposed to mild uncoupling of mitochondria triggered by FCCP.

2,4-Dinitrophenol (DNP) also induces an ATGL/HSL-independent form of autophagy

In order to validate the data and to limit the possibility of side effects due to FCCP, the effects of the incubation in the presence of one of two additional mitochondrial uncouplers, DNP, another proton ionophore (Bakker *et al.*, 1974) and the recently characterized C12TPP, a mitochondria-targeted ionophore (Kalinovich *et al.*, 2015), were assessed. Adipocytes exposed to either DNP (50 µM) or to C12TPP (1 µM) release more glycerol than control differentiated cells (**Fig. 7A, Supp. Fig. 3**, respectively). These data are comparable to those observed for cells exposed to FCCP and support the fact that the release is caused by mitochondrial uncoupling and not putative side effects (cytotoxicity,…) of FCCP. We next sought to determine whether the lipolysis induced by DNP relies on the same molecular machinery than the lipolysis triggered by FCCP. Interestingly, DNP-induced lipolysis is also

independent from ATGL- and HSL-mediated lipolysis. Indeed, the total protein abundance of these enzymes also decreases in adipocytes exposed FCCP (**Fig. 7B**). Moreover, as for FCCP, E600 did not prevent DNP-induced lipolysis (**Fig. 7A**) and glycerol release by DNP is also dependent on microautophagy, as it is significantly repressed in the presence of valinomycin (**Fig. 7C**).

Discussion

The present study demonstrates that a mild uncoupling of mitochondria induced by FCCP in murine 3T3-L1 adipocytes can significantly reduce their TAG content and is accompanied by a significant increase in glycerol and FFAs release into the extracellular conditioned culture medium, which is an indicator of activation of a form of lipolysis (Lass *et al.*, 2011). In addition, comparable effects on glycerol release were observed for 3 different compounds (FCCP, DNP and C12TPP), including one that has been characterized as a new uncoupler that specifically targets mitochondria (C12TPP) (Kalinovich and Shabalina, 2015). These data support the fact that the glycerol release by adipocytes exposed to uncouplers is a response to mitochondria uncoupling and not caused by a non-specific effect of FCCP.

These results are in agreement with previous results and data showing an increase in glycerol release in response to the overexpression of UCP-1 in 3T3-L1 murine adipocytes (Si *et al.*, 2007). Indeed, it has been reported that many biological adipocyte responses are comparable between FCCP addition and UCP-1 expression – both induce a decrease in adipocyte TAG content by promoting lipolysis and by decreasing lipid synthesis (Senocak *et al.*, 2007; Si *et al.*, 2007; Si *et al.*, 2009; Tejerina *et al.*, 2009); in addition, UCP-1 overexpression and FCCP down-regulate aerobic ATP production by mitochondria and increase oxygen consumption (Si *et al.*, 2007; Si *et al.*, 2009); and finally, both glucose uptake and glycolysis are stimulated in

the presence of FCCP or in response to UCP-1 overexpression (Si *et al.*, 2007; Si *et al.*, 2009). As we observed that FCCP (even used at 0.5 μM) can slightly decrease the viability of 3T3-L1 adipocytes (**Supp. Fig. 1A,B**), we cannot completely rule out the possibility that a small fraction of the glycerol released by FCCP-treated cells might be due to moderate cytotoxic effect of FCCP. However, it is unlikely that membrane damage possibly induced by FCCP could lead to glycerol release as a chemical permeabilization of the plasma membrane, by Triton X-100, does not lead to a measurable release of glycerol (data not shown).

The originality of the results presented here is based on the fact that mitochondrial uncoupling-induced glycerol release is not dependent on the classical enzyme machinery (HSL and ATGL) controlling lipolysis, as observed for the activation of lipolysis in adipocytes induced by either TNFα or isoproterenol (Kim *et al.*, 2006; Yang *et al.*, 2011). Indeed, in FCCP-treated cells, the abundance of both HSL and ATGL is reduced. In addition, the phosphorylation of serine 563, a residue targeted by PKA allowing the activation of HSL, could not be detected no matter what the condition of interest (data not shown), while the phosphorylation of serine 660, another marker of PKA-dependent HSL activation (Anthonsen *et al.*, 1998), was not significantly decreased in 3T3-L1 adipocytes incubated with FCCP, as previously observed (Tejerina *et al.*, 2009). However, the phosphorylation of HSL on serine 660 is increased in skeletal muscle of UCP-1-Tg mice (Keipert *et al.*, 2014). As FCCP addition and UCP-1 overexpression are supposed to trigger comparable cell responses in 3T3-L1 cells (Si *et al.*, 2009), this discrepancy could reflect either the existence of possible differences originating from the nature of the mitochondrial uncoupling or a cell type-based difference in the response to the uncoupling of mitochondria between adipocytes and muscle cells. Phosphorylation of HSL on serine 565 (mediated by AMPK) was not evaluated as AMPK does not regulate HSL activity in 3T3-L1 adipocytes (Watt *et al.*, 2006).

The expression of genes encoding HSL and ATGL is controlled by peroxisome proliferator-activated receptor γ (PPARγ) in rodent adipocytes, both *in vivo* and *in vitro* (Kershaw *et al.*, 2007; Kim *et al.*, 2006; Teruel *et al.*, 2005). The reduced abundance of HSL observed in FCCP-treated adipocytes could thus be explained by the decrease in the activity of PPARγ observed in adipocytes exposed to the uncoupler (Tejerina *et al.*, 2009).

In order to determine whether the activity of these enzymes contributes to the activation of lipolysis in FCCP-treated adipocytes, the effect of E600, an inhibitor of neutral lipases (Hermoso *et al.*, 1996), on the release of glycerol by FCCP-treated cells was tested. In agreement with the hypothesis presented above, E600 did not prevent FCCP-induced glycerol release, while it almost completely inhibits glycerol release by adipocytes stimulated with either TNFα or isoproterenol **(Fig. 2A)**. These results strongly support the fact that mitochondrial uncoupling-induced glycerol release does not rely on classical lipolysis mediated by HSL and ATGL.

The possibility of macroautophagy playing a role in this process was therefore explored. Indeed, Singh *et al.* (Singh *et al.*, 2009a) identified lipophagy as a new form of macroautophagy that specifically targets LDs. It is also been reported that a slight overexpression of *Atg5* is sufficient to activate macroautophagy and to decrease the weight of mice, emphasizing a possible role for macroautophagy in lipid disposal (Pyo *et al.*, 2013). Interestingly, the Lippincott-Schwartz group has recently and elegantly discussed the question of how cells and organisms adapt cellular FA flow and storage to changing nutrient availability and metabolic demand (Rambold *et al.*, 2015). These authors show that the use of cytosolic lipases versus lipophagy in lipid metabolism might be tissue and condition specific as mammalian cells use lipolysis during acute starvation to feed mitochondria with FAs, while serum depletion in the presence of glucose and amino acids up-regulates lipophagy (Rambold *et al.*, 2015). In addition, it has been suggested that the release of FAs from LDs by

macroautophagy could be of importance in cell types with low lipase activity such as hepatocytes (Singh *et al.*, 2009a) or, possibly, in the experimental conditions in which adipocytes exposed to mitochondrial uncoupling displayed a decrease in HSL and ATGL activity, which can be explained by a reduced PPARγ activity (Tejerina *et al.*, 2009).

In accordance with a possible role of macroautophagy in FCCP-induced glycerol release by 3T3-L1 adipocytes, macroautophagy seems stimulated in 3T3-L1 adipocytes exposed to the mitochondrial uncoupler. It is very likely that the increase in macroautophagy in these conditions is set up to degrade mitochondria by mitophagy, a biological process activated in order to deal with the stress (and usually mitochondrial network fragmentation) induced by the mitochondrial uncoupler, as previously demonstrated in HeLa cells (Wang *et al.*, 2012). However, it must be noted that the FCCP concentration used herein is much lower (0.5 µM) than the one used to trigger mitophagy (10 µM) by Wang *et al.*, and therefore only slightly affects cell viability (**Supp. Fig. 1A,B**). Mechanistically, autophagy activation by FCCP could also most likely be explained by the activation of AMPK as observed in adipocytes exposed to FCCP (data not shown) or in white adipose tissue of mice that overexpress UCP-1 in this tissue (Matejkova *et al.*, 2004).

While Singh and collaborators found a role for Atg5 in the activation of lipophagy in rat hepatocytes incubated in the presence of lipid-rich medium (Singh *et al.*, 2009a), in our experimental conditions, the silencing of either *Atg5* and/or *Atg7* does not prevent the FCCP-induced glycerol release in adipocytes, suggesting that the molecular mechanisms involved are likely to be different. However, it is possible that the efficiency of *Atg5*/*Atg7* silencing might not be strong enough to alter macroautophagy flow, an argument supported by the fact that this condition barely modifies the abundance of LC3-II and p62 in adipocytes while the silencing of *Atg7* is fully efficient in preadipocytes (**Fig. 3C-D**). However, the silencing of *Atg5* alone does not affect LC3-II and p62 abundance on preadipocytes either (**Fig. 3C**). This

apparent discrepancy between adipocytes and preadipocytes is in accordance with a recent study demonstrating a decrease in autophagy flow in differentiated adipocytes when compared to preadipocytes (Skop *et al.*, 2014). Another possibility would be that the form of autophagy activated by the uncoupling of mitochondria in 3T3-L1 adipocytes is independent of the molecular machinery classically involved in autophagy. Indeed, the existence of several forms of autophagy independent of Atg5 and/or Atg7 has been proposed recently. For instance, the silencing of these genes in MEFs is rescued by the activation of an alternative form of macroautophagy that is dependent on both Ulk-1 and Beclin-1 (Nishida *et al.*, 2009). More recently, the absolute requirement of Atg conjugation systems for formation of autophagosomes has also been questioned (Tsuboyama *et al.*, 2016). Indeed, the silencing of *Atg3*, *Atg5* and *Atg7* expression does not prevent the generation of syntaxin 17–positive autophagosome-like structures in starved MEFs, suggesting that some forms of autophagy could rely on other proteins (Tsuboyama *et al.*, 2016). Futures studies should thus be conducted in order to identify the molecular mechanisms involved in the autophagy activated by mitochondrial uncoupling in adipocytes.

In order to circumvent this problem and assess the role of autophagy in the FCCP-induced glycerol release, we used Baf A1, a V_0/V_1 H^+-ATPase inhibitor to inhibit macroautophagy (Yamamoto *et al.*, 1998). However, this compound had no inhibitory effect on the release of glycerol by adipocytes exposed to FCCP, while it efficiently increases the abundance of LC3-II used as a marker of autophagosome accumulation in both preadipocytes and adipocytes (Klionsky *et al.*, 2016) (**Fig. 3A**). The activation of lipolysis triggered in this condition could possibly be explained by the induction of a mild mitochondrial uncoupling induced by Baf A1, as demonstrated in murine RAW 264.7 macrophages, an effect that seems to be dependent on nitric oxide production in this cell type (Hong *et al.*, 2006). The reduction of mitochondrial membrane potential in response to Baf A1 has also been demonstrated in

human colon cancer cells (Zhdanov *et al.*, 2012), rat pheochromocytoma cells and human neuroblasts (Zhdanov *et al.*, 2011). Interestingly, while we did not find any inhibitory role for macroautophagy in FCCP-treated cells, this form of autophagy could possibly play a role in the basal lipolysis. Indeed, we observed a non-negligible co-localization between autophagosomes and lysosomes by confocal microscopy in untreated cells (**Supp. Fig. 4**). However, this level of co-localization is not significantly modified by the incubation in presence of FCCP (**Supp. Fig. 4**).

As a role for macroautophagy in glycerol release triggered by mitochondrial uncoupling was not conclusive, the role of lysosomes by another form of autophagy, such as microautophagy, was assessed. This form of autophagy consists in the direct capture of small cytosolic portions by the lysosomes and can either be non-selective or selective for some organelles as demonstrated for mitochondria (Lemasters, 2014), peroxisomes (Sakai *et al.*, 1998), nuclei (Dawaliby and Mayer, 2010), and ribosomes (Kraft *et al.*, 2008), although this process remains poorly documented in mammals. Recently, it was shown that incubation of yeast in lipid-rich medium leads to the specific activation of microautophagy selecting LDs (van Zutphen *et al.*, 2014). Others also demonstrated the existence of LD degradation by microautophagy in yeast during the stationary phase (Wang *et al.*, 2014). In this study, the uncoupler can increase the co-localization between lysosomes and LDs. Moreover, when the lysosomal function is altered by a combination of several molecules reported to poison the organelle (Baf A1 (Yamamoto *et al.*, 1998), NH_4Cl (Sun *et al.*, 2015), sucrose (DeCourcy *et al.*, 1991; Montgomery *et al.*, 1991), chloroquine (Sewell *et al.*, 1983), E64d (Ueno *et al.*, 1999)), an almost complete inhibition of the increase in glycerol released by FCCP-treated adipocytes was observed, suggesting a direct role for lysosomes in this process. Valinomycin, an inhibitor of microautophagy also recapitulates the effect of the lysosomal inhibitor cocktail. In conclusion, the glycerol released by adipocytes in response to exposure to

mitochondrial uncoupling depends essentially on a form of autophagy that seems to target LDs and microautophagy could possibly be involved in this process.

As expected and in accordance with previous studies, glycerol release induced by a mild mitochondrial uncoupling is accompanied by a release of FFA. It is thus unlikely that FFAs that are released are used to feed FFA β-oxidation in mitochondria as this metabolic pathway was not activated in adipocytes exposed to a mild uncoupling of mitochondria (De Pauw *et al.*, 2012), suggesting that, *in vivo*, FFAs could be released and that β-oxidation could take place in other tissues such as skeletal muscles (Turner *et al.*, 2014). Moreover, this hypothesis is in agreement with the recent findings that the efficient delivery of FFAs into mitochondria is dependent on mitochondrial fusion dynamics (Rambold *et al.*, 2015). Indeed, in mouse embryonic fibroblasts isolated from Mitofusin 1 knock-out mice that display fragmented mitochondria, a phenotype also observed in adipocytes facing mitochondrial uncoupling (De Pauw *et al.*, 2012), FFAs are heterogeneously distributed in the fragmented mitochondria, their metabolism is reduced, and more FFAs are fluxed out of the cells (Rambold *et al.*, 2015).

The molecular link existing between a mild mitochondrial uncoupling and the induction of a of microautophagy is not clear yet. Recently, several studies have reported a possible role for FOXO1 (Forkhead Homeobox type O 1) in the regulation of UCPs expression in 3T3-L1 adipocytes (Lettieri Barbato *et al.*, 2013; Liu *et al.*, 2016a; Liu *et al.*, 2016b), an effect dependent on the interaction between FOXO1 and TFEB (Transcription Factor EB). The same authors also demonstrated that FOXO1 is involved in the increased autophagy rate observed during adipogenesis, a process dependent on the positive effect of FOXO1 on the expression of the gene encoding Fsp2, a lipid droplet protein (Liu *et al.*, 2016b). Another research group also confirmed the upregulation of FOXO1 in 3T3-L1 adipocytes exposed to nutrient starvation. In this study, they identified that increase in FOXO1 expression was accompanied

by an increase in lysosomal lipase A expression and by a stronger co-localization between lipid droplets and lysosomes. The authors also evidenced that FFAs released by LIPA (Lysosomal Acid Lipase A) could be directed toward AMPK-mediated mitochondrial fatty acid β-oxidation (Lettieri Barbato *et al.*, 2013). It is tempting to speculate that these mechanisms could also be affected in our experimental conditions. However, despite a clear activation of AMPK (data not shown), we were not able to find any role for FOXO1 or LIPA in the FCCP-induced glycerol release (data not shown).

In conclusion, a form of autophagy seems to specifically target LDs in adipocytes exposed to a "mild" but chronic uncoupling of mitochondria. Future work studying the molecular mechanisms that mediate autophagy as well as the partitioning and fate of released FFAs should bring new information on TAG breakdown in many metabolic and lipid-associated diseases, such as obesity, diabetes and several cancers, in which the roles of lipid metabolism and mitochondrial dysfunction have been recently highlighted.

LDH release

Following incubation, LDH activity was assessed by using an enzymatic assay (Cytotoxicity Detection Kit; LDH, Roche) in conditioned media; detached cells and cell lysates were prepared by homogenization of the cells in 1 mL of PBS containing 10 % Triton X-100 (Merck), according to the manufacturer's instructions. The results were calculated as percentages of total LDH content released in the conditioned medium by using the following formula: $100 \times (a + b)/(a + b + c)$, where a is the supernatant LDH, b is the detached cells' LDH, and c is the adherent cells' LDH.

Cell viability assay

Cells were incubated in the presence of 500 µL of PBS containing 3-(4,5-dimethylthiazol-2-yl)-2,5-diphenyltetrazolium bromide (Sigma, 2.5 mg/mL). After 2 h of incubation at 37 °C, the conversion of this molecule into formazan was assessed by measuring absorbance with a spectrophotometer (570 nm). The results, obtained as absorbance units, were then normalized for protein content, as determined by the BCA method and as mentioned above.

Acknowledgements

Stéphane Demine was a recipient of a FRIA (Fonds pour la Recherche dans l'Industrie et l'Agriculture) fellowship (Fonds de la Recherche Scientifique (FRS-FNRS), Brussels, Belgium) and Nagabushana Reddy was a recipient of a grant from UNamur-CERUNA. The authors thank M.H. Rider (de Duve Institute, Université Catholique de Louvain, Brussels, Belgium) for his help during the design of triglyceride lipase assay and A. Greenberg (Tufts University, Boston, MA) for the anti-perilipin 1 antibody. The authors are also grateful to FRS-FNRS for their financial support (Crédit de Recherche: 19497337) and C. Demazy and N. Ninane from the Research Technological Platform Morphology – Imaging (UNamur) for their essential help for the confocal microscopy.

References

Adler-Wailes DC *et al.* 2015. Analysis of variants and mutations in the human winged helix FOXA3 gene and associations with metabolic traits. International journal of obesity.

Adler J *et al.* 2010. Quantifying colocalization by correlation: the Pearson correlation coefficient is superior to the Mander's overlap coefficient. Cytometry Part A : the journal of the International Society for Analytical Cytology 77(8):733-742.

Anthonsen MW *et al.* 1998. Identification of novel phosphorylation sites in hormone-sensitive lipase that are phosphorylated in response to isoproterenol and govern activation properties in vitro. The Journal of biological chemistry 273(1):215-221.

Arner P *et al.* 2011. Dynamics of human adipose lipid turnover in health and metabolic disease. Nature 478(7367):110-113.

Bakker EP *et al.* 1974. The binding of uncouplers of oxidative phosphorylation to rat-liver mitochondria. Biochimica et biophysica acta 333(1):12-21.

Bandyopadhyay U *et al.* 2008. The chaperone-mediated autophagy receptor organizes in dynamic protein complexes at the lysosomal membrane. Molecular and cellular biology 28(18):5747-5763.

Bjorkoy G *et al.* 2005. p62/SQSTM1 forms protein aggregates degraded by autophagy and has a protective effect on huntingtin-induced cell death. The Journal of cell biology 171(4):603-614.

Clement K *et al.* 1998. A mutation in the human leptin receptor gene causes obesity and pituitary dysfunction. Nature 392(6674):398-401.

Cuervo AM *et al.* 1997. A population of rat liver lysosomes responsible for the selective uptake and degradation of cytosolic proteins. The Journal of biological chemistry 272(9):5606-5615.

Dawaliby R *et al.* 2010. Microautophagy of the nucleus coincides with a vacuolar diffusion barrier at nuclear-vacuolar junctions. Molecular biology of the cell 21(23):4173-4183.

De Pauw A *et al.* 2012. Mild mitochondrial uncoupling does not affect mitochondrial biogenesis but downregulates pyruvate carboxylase in adipocytes: role for triglyceride content reduction. American journal of physiology Endocrinology and metabolism 302(9):E1123-1141.

DeCourcy K *et al.* 1991. Osmotic swelling of endocytic compartments induced by internalized sucrose is restricted to mature lysosomes in cultured mammalian cells. Experimental cell research 192(1):52-60.

Delaive E *et al.* 2008. A sensitive three-step protocol for fluorescence-based Western blot detection. Journal of immunological methods 334(1-2):51-58.

Demine S *et al.* 2012. Macroautophagy and cell responses related to mitochondrial dysfunction, lipid metabolism and unconventional secretion of proteins. Cells 1(2):168-203.

Doco-Fenzy M *et al.* 2014. Early-onset obesity and paternal 2pter deletion encompassing the ACP1, TMEM18, and MYT1L genes. European journal of human genetics : EJHG 22(4):471-479.

Dunn KW *et al.* 2011. A practical guide to evaluating colocalization in biological microscopy. American journal of physiology Cell physiology 300(4):C723-742.

Edens NK *et al.* 1990. Mechanism of free fatty acid re-esterification in human adipocytes in vitro. Journal of lipid research 31(8):1423-1431.

Fuller KM *et al.* 2003. Analysis of individual acidic organelles by capillary electrophoresis with laser-induced fluorescence detection facilitated by the endocytosis of fluorescently labeled microspheres. Analytical chemistry 75(9):2123-2130.

Furuchi T *et al.* 1993. Bafilomycin A1, a specific inhibitor of vacuolar-type H(+)-ATPase, blocks lysosomal cholesterol trafficking in macrophages. The Journal of biological chemistry 268(36):27345-27348.

Gilham D *et al.* 2003. Inhibitors of hepatic microsomal triacylglycerol hydrolase decrease very low density lipoprotein secretion. FASEB journal : official publication of the Federation of American Societies for Experimental Biology 17(12):1685-1687.

Graham JM. 2002. Preparation of crude subcellular fractions by differential centrifugation. TheScientificWorldJournal 2:1638-1642.

Guh DP *et al.* 2009. The incidence of co-morbidities related to obesity and overweight: a systematic review and meta-analysis. BMC public health 9:88.

Hanada T *et al.* 2007. The Atg12-Atg5 conjugate has a novel E3-like activity for protein lipidation in autophagy. The Journal of biological chemistry 282(52):37298-37302.

Harper JA *et al.* 2001. Mitochondrial uncoupling as a target for drug development for the treatment of obesity. Obesity reviews : an official journal of the International Association for the Study of Obesity 2(4):255-265.

Hermoso J *et al.* 1996. Lipase activation by nonionic detergents. The crystal structure of the porcine lipase-colipase-tetraethylene glycol monooctyl ether complex. The Journal of biological chemistry 271(30):18007-18016.

Hong J *et al.* 2006. Nitric oxide production by the vacuolar-type (H+)-ATPase inhibitors bafilomycin A1 and concanamycin A and its possible role in apoptosis in RAW 264.7 cells. The Journal of pharmacology and experimental therapeutics 319(2):672-681.

Hosogai N *et al.* 2007. Adipose tissue hypoxia in obesity and its impact on adipocytokine dysregulation. Diabetes 56(4):901-911.

Hubbard VM *et al.* 2010. Macroautophagy regulates energy metabolism during effector T cell activation. Journal of immunology 185(12):7349-7357.

Jensen MD *et al.* 2001. Lipid metabolism during fasting. American journal of physiology Endocrinology and metabolism 281(4):E789-793.

Jones LR *et al.* 2007. Lifestyle modification in the treatment of obesity: an educational challenge and opportunity. Clinical pharmacology and therapeutics 81(5):776-779.

Kabeya Y *et al.* 2000. LC3, a mammalian homologue of yeast Apg8p, is localized in autophagosome membranes after processing. The EMBO journal 19(21):5720-5728.

Kalinovich AV *et al.* 2015. Novel Mitochondrial Cationic Uncoupler C4R1 Is an Effective Treatment for Combating Obesity in Mice. Biochemistry Biokhimiia 80(5):620-628.

Kaushik S *et al.* 2015. Degradation of lipid droplet-associated proteins by chaperone-mediated autophagy facilitates lipolysis. Nature cell biology 17(6):759-770.

Kaushik S *et al.* 2016. AMPK-dependent phosphorylation of lipid droplet protein PLIN2 triggers its degradation by CMA. Autophagy 12(2):432-438.

Kaushik S *et al.* 2011. Autophagy in hypothalamic AgRP neurons regulates food intake and energy balance. Cell metabolism 14(2):173-183.

Keipert S *et al.* 2014. Skeletal muscle mitochondrial uncoupling drives endocrine cross-talk through the induction of FGF21 as a myokine. American journal of physiology Endocrinology and metabolism 306(5):E469-482.

Kershaw EE *et al.* 2007. PPARgamma regulates adipose triglyceride lipase in adipocytes in vitro and in vivo. American journal of physiology Endocrinology and metabolism 293(6):E1736-1745.

Kim JY *et al.* 2006. The adipose tissue triglyceride lipase ATGL/PNPLA2 is downregulated by insulin and TNF-alpha in 3T3-L1 adipocytes and is a target for transactivation by PPARgamma. American journal of physiology Endocrinology and metabolism 291(1):E115-127.

Klionsky DJ *et al.* 2016. Guidelines for the use and interpretation of assays for monitoring autophagy (3rd edition). Autophagy 12(1):1-222.

Klionsky DJ *et al.* 2008. Does bafilomycin A1 block the fusion of autophagosomes with lysosomes? Autophagy 4(7):849-850.

Komatsu M *et al.* 2005. Impairment of starvation-induced and constitutive autophagy in Atg7-deficient mice. The Journal of cell biology 169(3):425-434.

Kong LC *et al.* 2014. Dietary patterns differently associate with inflammation and gut microbiota in overweight and obese subjects. PloS one 9(10):e109434.

Kraft C *et al.* 2008. Mature ribosomes are selectively degraded upon starvation by an autophagy pathway requiring the Ubp3p/Bre5p ubiquitin protease. Nature cell biology 10(5):602-610.

Kunz JB *et al.* 2004. Determination of four sequential stages during microautophagy in vitro. The Journal of biological chemistry 279(11):9987-9996.

Lafontan M *et al.* 2009. Lipolysis and lipid mobilization in human adipose tissue. Progress in lipid research 48(5):275-297.

Lass A *et al.* 2006. Adipose triglyceride lipase-mediated lipolysis of cellular fat stores is activated by CGI-58 and defective in Chanarin-Dorfman Syndrome. Cell metabolism 3(5):309-319.

Lass A *et al.* 2011. Lipolysis - a highly regulated multi-enzyme complex mediates the catabolism of cellular fat stores. Progress in lipid research 50(1):14-27.

Lemasters JJ. 2014. Variants of mitochondrial autophagy: Types 1 and 2 mitophagy and micromitophagy (Type 3). Redox biology 2:749-754.

Lettieri Barbato D *et al.* 2013. FoxO1 controls lysosomal acid lipase in adipocytes: implication of lipophagy during nutrient restriction and metformin treatment. Cell death & disease 4:e861.

Liu L *et al.* 2016a. FoxO1 interacts with transcription factor EB and differentially regulates mitochondrial uncoupling proteins via autophagy in adipocytes. Cell death discovery 2:16066.

Liu L *et al.* 2016b. FoxO1 antagonist suppresses autophagy and lipid droplet growth in adipocytes. Cell cycle 15(15):2033-2041.

Martinez-Lopez N *et al.* 2016. Autophagy in the CNS and Periphery Coordinate Lipophagy and Lipolysis in the Brown Adipose Tissue and Liver. Cell metabolism 23(1):113-127.

Matejkova O *et al.* 2004. Possible involvement of AMP-activated protein kinase in obesity resistance induced by respiratory uncoupling in white fat. FEBS letters 569(1-3):245-248.

Maylie MF *et al.* 1972. Action of organophosphates and sulfonyl halides on porcine pancreatic lipase. Biochimica et biophysica acta 276(1):162-175.

Montgomery RR *et al.* 1991. Accumulation of indigestible substances reduces fusion competence of macrophage lysosomes. Journal of immunology 147(9):3087-3095.

Nishida Y *et al.* 2009. Discovery of Atg5/Atg7-independent alternative macroautophagy. Nature 461(7264):654-658.

Pearson GL *et al.* 2014. Lysosomal acid lipase and lipophagy are constitutive negative regulators of glucose-stimulated insulin secretion from pancreatic beta cells. Diabetologia 57(1):129-139.

Pyo JO *et al.* 2013. Overexpression of Atg5 in mice activates autophagy and extends lifespan. Nature communications 4:2300.

Rambold AS *et al.* 2015. Fatty Acid Trafficking in Starved Cells: Regulation by Lipid Droplet Lipolysis, Autophagy, and Mitochondrial Fusion Dynamics. Developmental cell.

Rider MH *et al.* 2011. AMP-activated protein kinase and metabolic regulation in cold-hardy insects. Journal of insect physiology 57(11):1453-1462.

Sahu-Osen A *et al.* 2015. CGI-58/ABHD5 is phosphorylated on Ser239 by protein kinase A: control of subcellular localization. Journal of lipid research 56(1):109-121.

Sakai Y *et al.* 1998. Peroxisome degradation by microautophagy in Pichia pastoris: identification of specific steps and morphological intermediates. The Journal of cell biology 141(3):625-636.

Schimmel RJ. 1976. Roles of alpha and beta adrenergic receptors in control of glucose oxidation in hamster epididymal adipocytes. Biochimica et biophysica acta 428(2):379-387.

Senocak FS *et al.* 2007. Effect of uncoupling protein-1 expression on 3T3-L1 adipocyte gene expression. FEBS letters 581(30):5865-5871.

Sewell RB *et al.* 1983. Effect of chloroquine on the form and function of hepatocyte lysosomes. Morphologic modifications and physiologic alterations related to the biliary excretion of lipids and proteins. Gastroenterology 85(5):1146-1153.

Si Y *et al.* 2007. Effects of forced uncoupling protein 1 expression in 3T3-L1 cells on mitochondrial function and lipid metabolism. Journal of lipid research 48(4):826-836.

Si Y *et al.* 2009. Metabolic flux analysis of mitochondrial uncoupling in 3T3-L1 adipocytes. PloS one 4(9):e7000.

Singh R *et al.* 2009a. Autophagy regulates lipid metabolism. Nature 458(7242):1131-1135.

Singh R *et al.* 2009b. Autophagy regulates adipose mass and differentiation in mice. The Journal of clinical investigation 119(11):3329-3339.

Skop V *et al.* 2014. Autophagy inhibition in early but not in later stages prevents 3T3-L1 differentiation: Effect on mitochondrial remodeling. Differentiation; research in biological diversity 87(5):220-229.

Souza SC *et al.* 2002. Modulation of hormone-sensitive lipase and protein kinase A-mediated lipolysis by perilipin A in an adenoviral reconstituted system. The Journal of biological chemistry 277(10):8267-8272.

Spangenburg EE *et al.* 2011. Use of BODIPY (493/503) to visualize intramuscular lipid droplets in skeletal muscle. Journal of biomedicine & biotechnology 2011:598358.

Sprinthall RC. 2012. Basic statistical analysis. Boston: Pearson Allyn & Bacon.

Sun K *et al.* 2011. Adipose tissue remodeling and obesity. The Journal of clinical investigation 121(6):2094-2101.

Sun R *et al.* 2015. Ammonium chloride inhibits autophagy of hepatocellular carcinoma cells through SMAD2 signaling. Tumour biology : the journal of the International Society for Oncodevelopmental Biology and Medicine 36(2):1173-1177.

Tanida I *et al.* 2001. The human homolog of Saccharomyces cerevisiae Apg7p is a Protein-activating enzyme for multiple substrates including human Apg12p, GATE-16, GABARAP, and MAP-LC3. The Journal of biological chemistry 276(3):1701-1706.

Tansey JT *et al.* 2003. Functional studies on native and mutated forms of perilipins. A role in protein kinase A-mediated lipolysis of triacylglycerols. The Journal of biological chemistry 278(10):8401-8406.

Tejerina S *et al.* 2009. Mild mitochondrial uncoupling induces 3T3-L1 adipocyte de-differentiation by a PPARgamma-independent mechanism, whereas TNFalpha-induced de-differentiation is PPARgamma dependent. Journal of cell science 122(Pt 1):145-155.

Teruel T *et al.* 2005. Rosiglitazone up-regulates lipoprotein lipase, hormone-sensitive lipase and uncoupling protein-1, and down-regulates insulin-induced fatty acid synthase gene expression in brown adipocytes of Wistar rats. Diabetologia 48(6):1180-1188.

Tsuboyama K *et al.* 2016. The ATG conjugation systems are important for degradation of the inner autophagosomal membrane. Science 354(6315):1036-1041.

Turner N *et al.* 2014. Fatty acid metabolism, energy expenditure and insulin resistance in muscle. The Journal of endocrinology 220(2):T61-79.

Ueno T *et al.* 1999. Autolysosomal membrane-associated betaine homocysteine methyltransferase. Limited degradation fragment of a sequestered cytosolic enzyme monitoring autophagy. The Journal of biological chemistry 274(21):15222-15229.

van Zutphen T *et al.* 2014. Lipid droplet autophagy in the yeast Saccharomyces cerevisiae. Molecular biology of the cell 25(2):290-301.

Vankoningsloo S *et al.* 2006. CREB activation induced by mitochondrial dysfunction triggers triglyceride accumulation in 3T3-L1 preadipocytes. Journal of cell science 119(Pt 7):1266-1282.

Vankoningsloo S *et al.* 2005. Mitochondrial dysfunction induces triglyceride accumulation in 3T3-L1 cells: role of fatty acid beta-oxidation and glucose. Journal of lipid research 46(6):1133-1149.

Wabitsch M *et al.* 2015. Biologically inactive leptin and early-onset extreme obesity. The New England journal of medicine 372(1):48-54.

Wang CW *et al.* 2014. A sterol-enriched vacuolar microdomain mediates stationary phase lipophagy in budding yeast. The Journal of cell biology 206(3):357-366.

Wang Y *et al.* 2012. ROS-induced mitochondrial depolarization initiates PARK2/PARKIN-dependent mitochondrial degradation by autophagy. Autophagy 8(10):1462-1476.

Watt MJ *et al.* 2006. Regulation of HSL serine phosphorylation in skeletal muscle and adipose tissue. American journal of physiology Endocrinology and metabolism 290(3):E500-508.

Wattiaux R *et al.* 1978. Isolation of rat liver lysosomes by isopycnic centrifugation in a metrizamide gradient. The Journal of cell biology 78(2):349-368.

Wei E *et al.* 2007. Attenuation of adipocyte triacylglycerol hydrolase activity decreases basal fatty acid efflux. The Journal of biological chemistry 282(11):8027-8035.

Yamamoto A *et al.* 1998. Bafilomycin A1 prevents maturation of autophagic vacuoles by inhibiting fusion between autophagosomes and lysosomes in rat hepatoma cell line, H-4-II-E cells. Cell structure and function 23(1):33-42.

Yang X *et al.* 2011. Relative contribution of adipose triglyceride lipase and hormone-sensitive lipase to tumor necrosis factor-alpha (TNF-alpha)-induced lipolysis in adipocytes. The Journal of biological chemistry 286(47):40477-40485.

Yin J *et al.* 2009. Role of hypoxia in obesity-induced disorders of glucose and lipid metabolism in adipose tissue. American journal of physiology Endocrinology and metabolism 296(2):E333-342.

Yoshimori T *et al.* 1991. Bafilomycin A1, a specific inhibitor of vacuolar-type H(+)-ATPase, inhibits acidification and protein degradation in lysosomes of cultured cells. The Journal of biological chemistry 266(26):17707-17712.

Zhang Y *et al.* 2009. Adipose-specific deletion of autophagy-related gene 7 (atg7) in mice reveals a role in adipogenesis. Proceedings of the National Academy of Sciences of the United States of America 106(47):19860-19865.

Zhdanov AV *et al.* 2011. Bafilomycin A1 activates respiration of neuronal cells via uncoupling associated with flickering depolarization of mitochondria. Cellular and molecular life sciences : CMLS 68(5):903-917.

Zhdanov AV *et al.* 2012. Bafilomycin A1 activates HIF-dependent signalling in human colon cancer cells via mitochondrial uncoupling. Bioscience reports 32(6):587-595.

Figure legends

Figure 1: Effect of a mild mitochondrial uncoupling on glycerol release, TAG content and FFA release.

Preadipocytes were differentiated into adipocytes over 12 days and incubated in culture medium containing 10 % FBS, with (FCCP, grey columns) or without 0.5 µM of FCCP (CTL, white columns) for 3 days. Culture media were renewed every 24 h. **A.** Concentration of glycerol released into conditioned culture media was determined using the TAG and free glycerol assay kit. Results were normalized for protein content and are expressed in µg of glycerol released per mg of proteins, and represent means ± s.d. (n=3 independent experiments). *p<0.05: significantly different from CTL as determined by the Student *t*-test. **B.** TAG content of cells was determined using the TAG and free glycerol assay kit. Results are normalized for protein content, expressed in µg of TAG/µg of adipocyte proteins as means ± s.d. (n=8 independent experiments). *p<0.05: significantly different from control as determined by the Student *t*-test. **C.** Representative micrographs of both control and FCCP-treated adipocytes are presented on the left of the corresponding chart (magnification, 25×). **D.** Release of FFAs from cells treated as described above was determined using the FFA assay kit. As a control, some cells were treated for 24 h with 10 µM isoproterenol (ISO). Results are normalized for protein content, expressed in µmole of FFAs/mg of adipocyte proteins as means ± s.d. (n=6 independent experiments). *p<0.05: significantly different from control as determined by the Student *t*-test.

Figure 2: Effect of a mild mitochondrial uncoupling on molecular actors regulating canonical lipolysis.

A. Cells were differentiated for 12 days (CTL, white columns) and treated with either 0.5 µM of FCCP (grey columns), 10 ng/mL of TNFα (black columns), or 10 µM of isoproterenol (light grey columns) for 3 days. When indicated, E600 (10 µM, squared columns) was added during the last 24 h of incubation. Conditioned culture media were collected and glycerol concentration was determined. Results were normalized for protein content and are expressed in µg of glycerol released per mg of proteins and represent means ± s.d. (n=3 independent experiments). **p<0.01, ***p<0.001: means were significantly different as determined by one-way ANOVA with Tukey test. **B.** Fluorescence-based western blot analysis and quantification of the abundance of total HSL, phosphorylated HSL (p-Ser660), ATGL, and perilipin 1. Equal protein loading was controlled by the immunodetection of α-tubulin. The fluorescence intensity of each band of interest was quantified and normalized for α-tubulin signals. For HSL phosphorylation, signals obtained for the phosphorylated form were first normalized for the total HSL protein abundance and then for the loading control (α-tubulin signal). Results are expressed in percentages of control cells and presented as means ± s.d. (n=4 independent experiments). *p<0.05, ***p<0.01, significantly different from control as determined by the Student *t*-test; ns: no significant difference from control. **C.** Cells were differentiated for 12 days and treated with 0.5 µM of FCCP (FCCP, grey columns) or without (CTL, white columns) for a further 3 days. Media were renewed every 24 h. When indicated, E600 (10 µM, squared columns) was added during the last 24 h of incubation. Total TAG lipase was assayed by measuring [9-10-^{3}H(N)]-triolein breakdown. Results are expressed as counts per minute and represent means ± s.d. (n=3 independent experiments). *p<0.05: significantly different from control as determined by one-way ANOVA with Tukey test.

Figure 3: Effect of macroautophagy inhibition on lipolysis in adipocytes exposed to mild uncoupling of mitochondria

A. Cells were differentiated and exposed or not to FCCP for 3 days as described above. When indicated, during the last 24 h of incubation, 400 µM Baf A1 was added to the cells. **A**. The abundance of LC3-II and p62 was analyzed on 25 µg of proteins of cleared cell lysates by fluorescence-based western blotting. For quantification, the fluorescence intensity of the bands of interest was normalized for paired signals corresponding to α-tubulin abundance. Results are expressed as percentages of control cells and represent means ± s.d. (n=4 independent experiments). *p<0.05, **p<0.01, the two conditions indicated by the black bar are significantly different, as determined by the *t*-test. ns: no significant difference existing between the conditions indicated by the black bar. **B,C,D**. Adipocytes (**B**,**C**) and preadipocytes (**D**) were transfected by electroporation in the presence of siRNA targeting Atg5 (20 nM), Atg7 (100 nM) (alone or in combination) or control siRNA (siNTP) (120 nM). After 24 h of recovery, cells were incubated in the presence or in the absence of 0.5 µM FCCP for 3 days. Cell culture media were renewed every day. **B**. At the end of the incubations, conditioned culture media were collected and glycerol concentration was determined. Results were normalized for protein content and are expressed in µg of glycerol released per mg of proteins and represent means ± s.d. (n=6 independent experiments). *p<0.05, mean is significantly different from the corresponding control as determined with one-way ANOVA with Tukey test; ns: not significantly different. **C,D**. After 3 days post-electroporation, the abundance of p62 and LC3-II proteins was analyzed by fluorescence-based western blotting on 25 µg of proteins prepared from cleared cell lysates. Equal protein loading was controlled by the immunodetection of α-tubulin. The fluorescence intensity of bands of interest was quantified and then normalized for paired signals corresponding to α-tubulin abundance. Results are expressed as percentages of cells electroporated with control

siRNA (siNTP) and represent means ± s.d. (C, n=3; D, n=2). **E.** Cells were differentiated and exposed or not to FCCP for 3 days as described above. When indicated, during the last 24 h of incubation, Baf A1 (400 µM) was added to the cells. Culture media were then collected and the glycerol concentration was determined. Normalized results for protein content are expressed in µg of glycerol released per mg of proteins and are presented as means ± s.d. (n=3 independent experiments). **p<0.01, means were significantly different as determined with one-way ANOVA with Tukey test; ns: not significantly different.

Figure 4: Mitochondrial uncoupling increases co-localization between lysosomes and lipid droplets

Cells were differentiated and exposed or not to FCCP for 3 days as described above. **A.** The co-localization between LDs and lysosomes was visualized by confocal microscopy in cells in which lysosomes, LDs, and nuclei were stained by LysoTracker Red (red), BODIPY 493/503 (green) and TO-PRO3 iodide (blue), respectively. White arrows indicate co-localization events between LDs and lysosomes. The size is indicated by the scale bar. **B.** Cells were differentiated and exposed or not to FCCP for 3 days as described above. During the last 24h of incubation, cells were incubated in presence of 400 µM Baf A1. At the end, lysosomes, LDs, and nuclei were detected by using antibodies targeting LAMP-1 (Alexa Fluor 488, green), perilipin 1 (Alexa Fluor 546, red) and TO-PRO3 iodide (blue), respectively. White arrows indicate co-localization events between LDs and lysosomes. Size is indicated by the scale bar. **C.** The co-localization between lysosomes stained with LysoTracker (**A**) and LDs was assessed in a quantitative manner by measuring the Pearson correlation coefficient (which compares the correlation between each fluorescence channel for each pixel of the micrograph) by using the ImageJ plugin Coloc2, as detailed in the materials and methods section (n = 15 (CTL) or 16 cells (FCCP). **p<0.01: significantly different from control as determined by the Student *t*-test. **D.** The co-localization between lysosomes and LDs from

experiment illustrated in **B**, was also assessed by using the method described above (n = 20 cells). **p<0.01: significantly different from control as determined by the Student *t*-test, ns: not significantly different.

Figure 5: Ultrastructure of adipocytes incubated in the presence of FCCP

Cells were differentiated and exposed or not (CTL) to FCCP for 3 days. At the end of the incubations, the ultrastructure of these cells was assessed by TEM as described in the "Materials and Methods" section. Black arrows indicate the close proximity events between endolysosomal vesicles and LDs. The scale is indicated on each micrograph. L: lipid droplet; N: nucleus; *: endolysosomal vesicle.

Figure 6: FCCP-induced lipolysis is prevented by lysosomal poisoning and inhibition of microautophagy

Cells were differentiated and exposed (grey columns) or not (white columns) to FCCP for 3 days as described above. **A.** Following the different treatments, lysosome-enriched fractions were prepared by ultracentrifugation according to the protocol described in the "Materials and Methods" section, and TAG concentration was determined using the free glycerol and TAG and glycerol assay kit. Results were normalized for protein content, and are expressed as µg of TAG per mg of proteins and represent means ± s.d. (n=3 independent experiments). **B, C.** In some conditions, during the last 24 h of treatment, 400 µM of Baf A1, 10 µg/mL of E64d, 10 mM of NH_4Cl, 10 µM of chloroquine (CLQ), and 10 mM of sucrose (Suc), or all the inhibitors mentioned above at the same time (All) (**B**) or 1 µM of valinomycin (valino, squared columns) (**C**) were added. Media were finally collected and the glycerol concentration was determined. Results were normalized for protein content, are expressed in µg of glycerol released per mg of proteins, and represent means ± s.d (n=3 independent experiments). **D.** During the last 24 h of treatment, 1 µM of valinomycin (valino, squared

columns) was added or not to adipocytes treated or not with FCCP. Lysosome-enriched fractions were then prepared according to the protocol described in the Materials and Methods section and kept at 37 °C for 1 h in a preserving buffer. Lysosomes were finally pelleted and the glycerol concentration was measured in the supernatants. Results were normalized for total protein content, are expressed as µg of glycerol released per mg of proteins, and represent means ± s.d. (n=4 independent experiments). *p<0.05, ***p<0.001: means were significantly different between the conditions indicated by the black line, as determined by the Student *t*-test (A) or one-way ANOVA with Tukey test (B–D); ns: not significantly different.

Figure 7: DNP triggers a form of lipolysis comparable to the one induced by FCCP

Adipocytes were incubated in culture medium containing 10 % FBS (CTL, white columns), with or without 0.5 µM of FCCP (FCCP, grey columns), or with or without 50 µM of DNP (DNP, black columns) for 3 days. Media were renewed every 24 h. **A.** During the last 24 h of incubation, 10 µM of E600 (squared columns) was added to some cells. The concentration of glycerol released into the conditioned culture media was determined using the TAG and free glycerol determination kit. The results were normalized for protein content and are expressed as µg of glycerol per mg of proteins, as means ± s.d. (n=3 independent experiments). **B.** Fluorescent western blot analysis and quantification of the abundance of total HSL, phosphorylated HSL (p-Ser660), and ATGL. Equal protein loading was controlled by the immunodetection of α-tubulin. The fluorescence intensity of each band of interest was measured and normalized for α-tubulin signals. For HSL phosphorylation, the signal obtained for the phosphorylated form was normalized first for the total HSL protein abundance and then for the α-tubulin signal. Results are expressed in percentages of differentiated cells and presented as means ± s.d. (n=3 independent experiments). **C.** During the last 24 h of incubation, 10 µM of valinomycin (squared columns) were added to some cells. The concentration of glycerol released into the conditioned culture media was determined using

the TAG and free glycerol determination kit. The results were normalized for protein content and are expressed as µg of glycerol per mg of proteins, as means ± s.d. (n=3 independent experiments). *$p<0.05$, **$p<0.01$, or ***$p<0.001$: means were significantly different from the control cells, as determined by one-way ANOVA with Tukey test. ns: not significantly different.

Figure 1

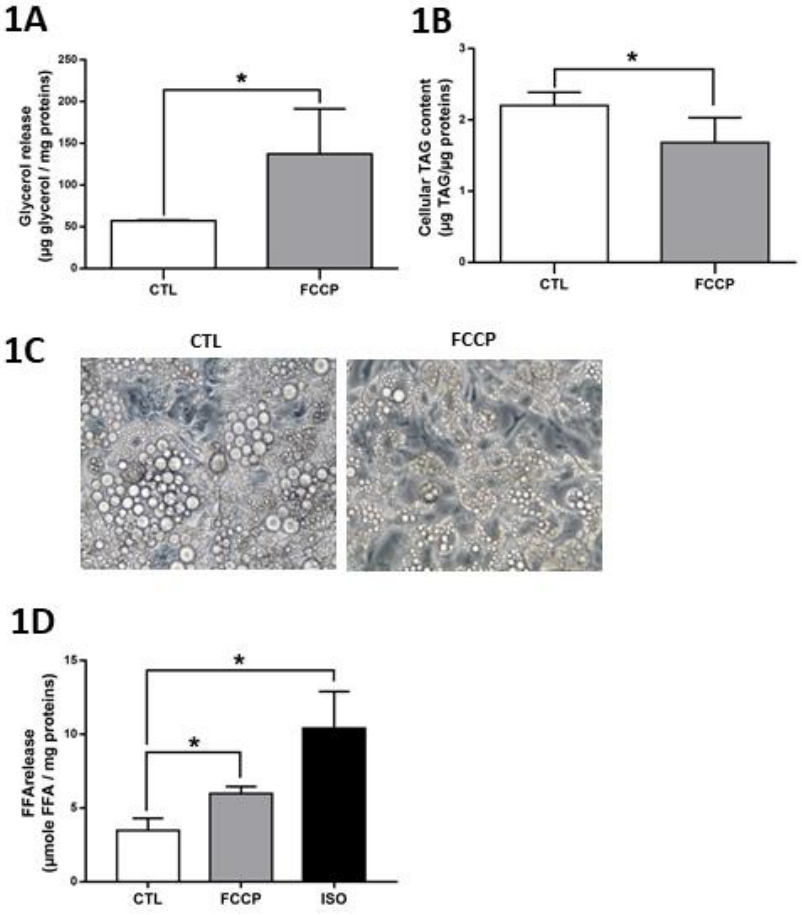

Figure 2

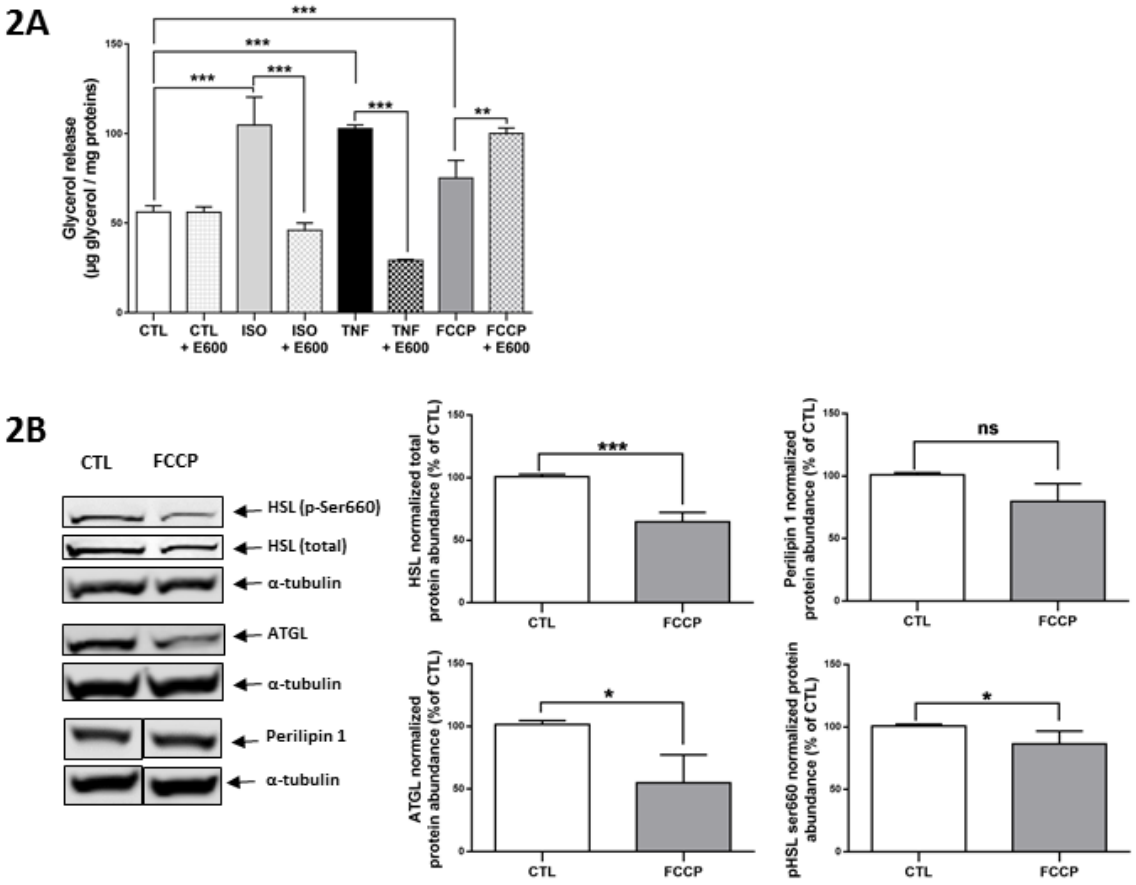

Figure 3

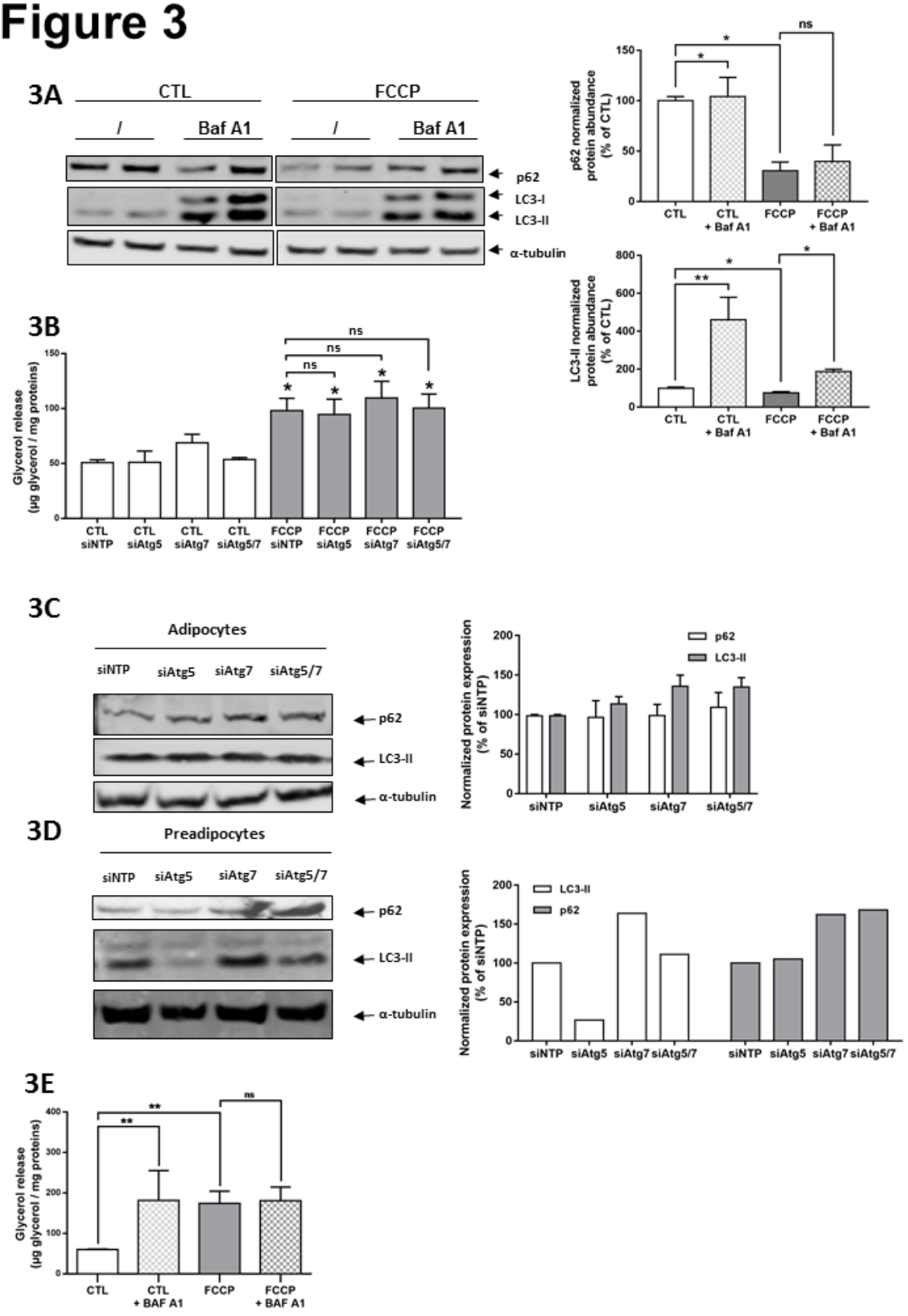

Figure 4

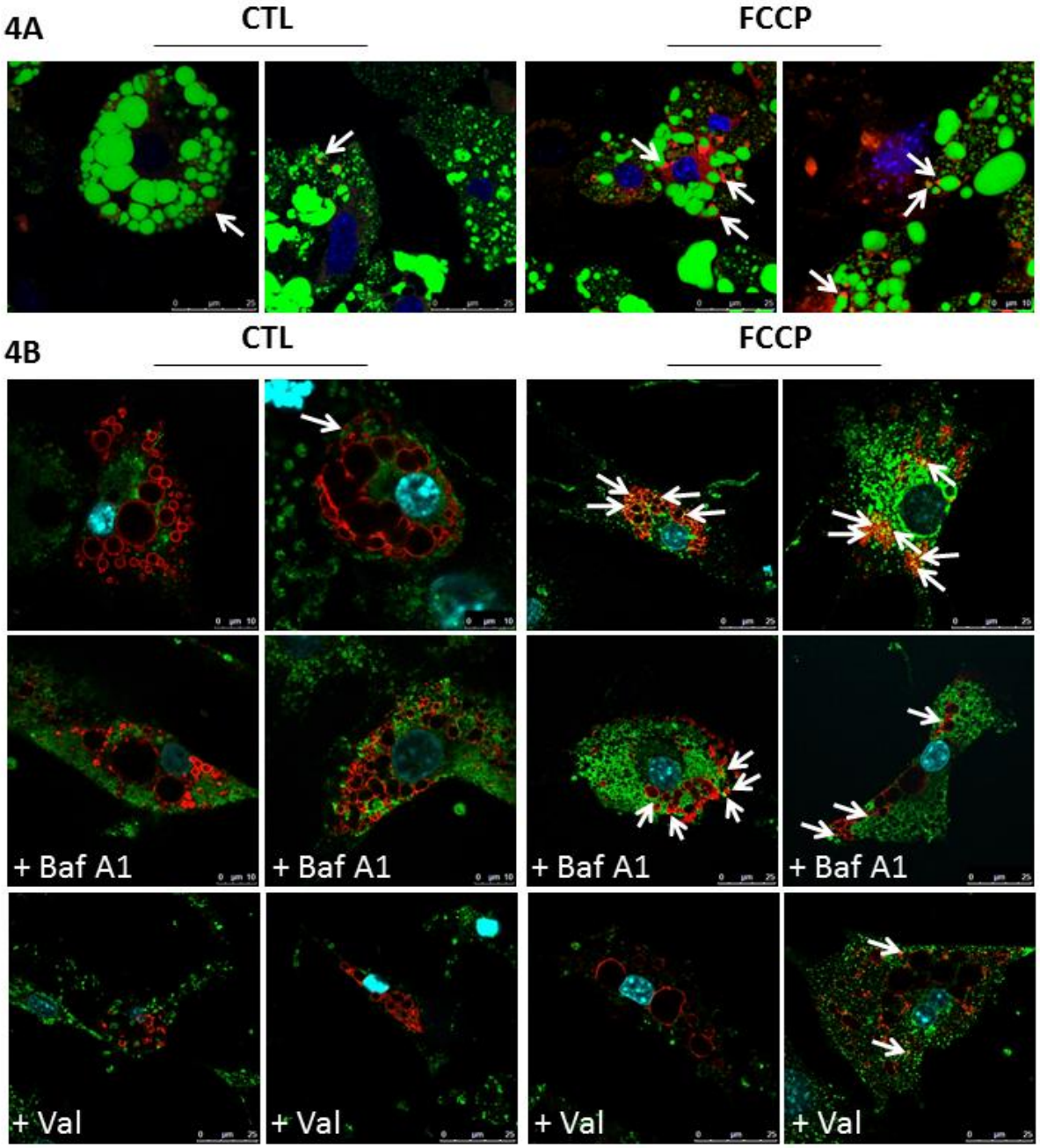

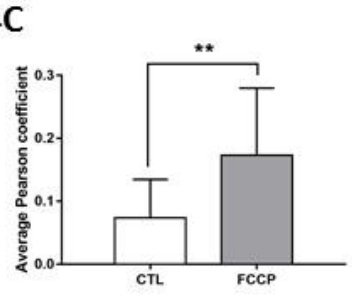

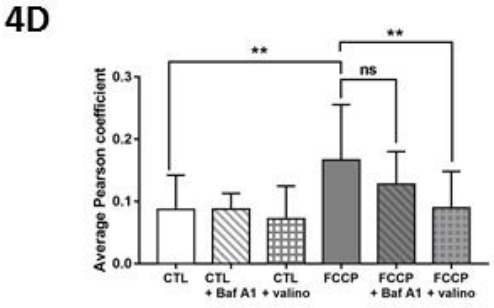

Figure 5

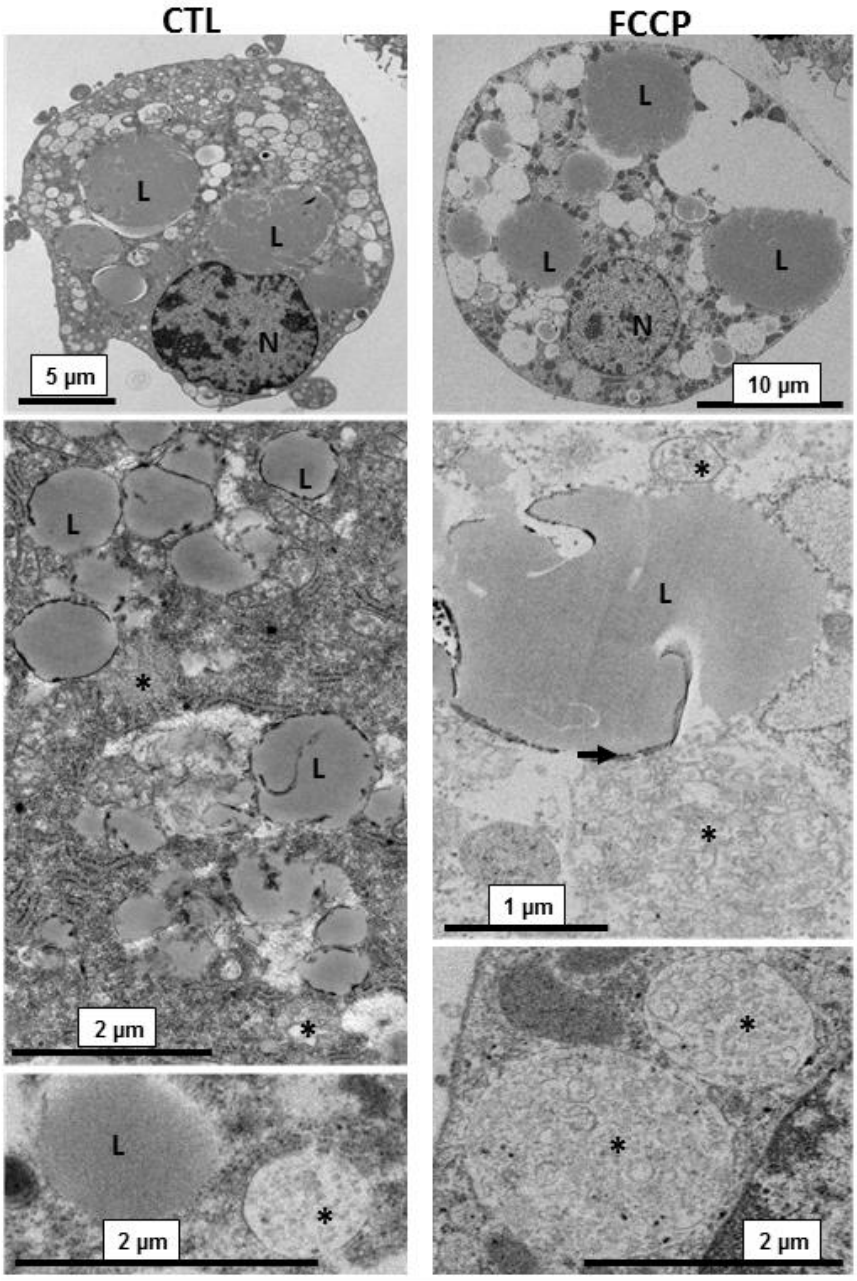

Conditions	Cells presenting autophagic vesicles in contact with lipid droplets (%)	Number of autophagic vesicles in contact with lipid droplets per cell
CTL	25 %	2.2 vesicles
FCCP	45 %	3.2 vesicles

Figure 6

6A

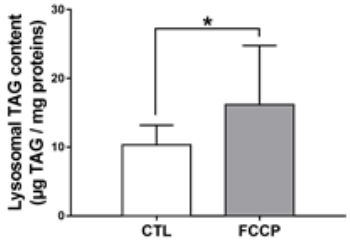

6B

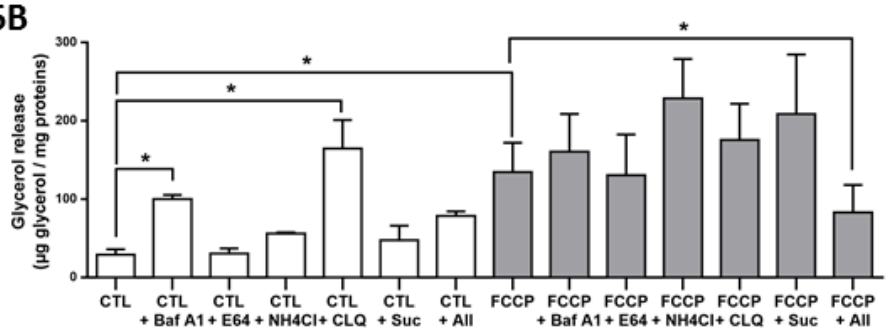

6C

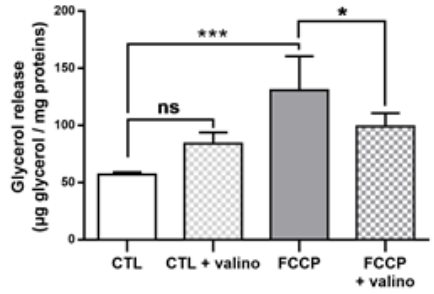

6D

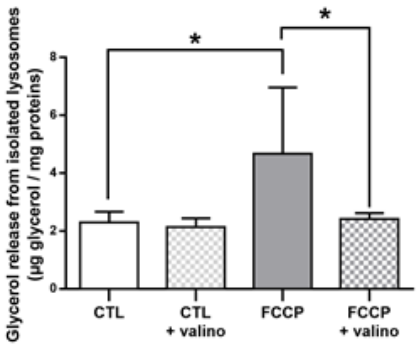

Figure 7